

Bluetooth® Low Energy Direction Finding and Measurement for Quality Assurance

Yoshihide Goto, Akihisa Kumaki, Takashi Nakano

[Summary] Bluetooth® technology supporting wireless devices such as headphones is being developed for new applications including direction finding and distance detection in addition to data transmission. Bluetooth technology is being used in a widening range of fields since the first standard was established over 20 years ago in 1998. Anritsu's MT8852B Bluetooth Test Set applies a comprehensive RF test environment for assuring BT hardware functions and has now been updated with firmware supporting the new Angle of Arrival (AoA) and Angle of Departure (AoD) specifications used by the direction finding function.

1 Introduction

Bluetooth® technology is used by many short-range wireless devices, such as headphones, speakers, smart watches, etc. This application range covers not only data transmission but also development of distance detection, direction finding, etc., with an ever-widening application range over the 20 years since the first standard was established in 1998.

Not only has the application range for Bluetooth technology become widespread, but a large ecosystem has also developed around connection testing events and certification testing to assure excellent interconnectivity between Bluetooth devices. Anritsu became a Bluetooth SIG member in 1999 and has participated actively in introduction of new standards and interconnectivity testing since then. The MT8852B Bluetooth Test Set (MT8852B hereafter) has been developed based on knowledge gained through these activities and is an irreplaceable tool for RF testing environments to assure Bluetooth hardware performance; it is used both for evaluating devices under development and for manufacturing-shipment inspections.

With functions for controlling Bluetooth devices at RF testing, the MT8852B is ideal for configuring a standalone measurement environment. This report introduces the functions of the MT8852B with particular focus on the added Bluetooth direction finding functions.



Figure 1 MT8852B Bluetooth Test Set

2 Evolution of Bluetooth Low Energy

The first Bluetooth standard covered the Basic Rate for telephone headsets, etc., at speeds of 1 Mbps and was subsequently extended as the Enhanced Data Rate (EDR) supporting faster data rates of 2 and 3 Mbps for such as music applications requiring higher speeds. Subsequently, the Bluetooth Low Energy (1 Mbps) standard was released for systems requiring longer battery life in contrast to wireless systems, such as mobile phones and wireless LAN (WLAN), targeting faster speeds.

2.1 What is Bluetooth Low Energy?

Bluetooth Low Energy simplifies the specifications in comparison to the Basic Rate and EDR specifications with the intention of reducing power consumption by adopting a configuration for flexible control of the communication timing. As a result, Remote devices such as temperature sensors can operate for periods of years using only a small “coin” battery. Additionally, increasing the number of simultaneous connections supports configuration of mesh networks aggregating many devices.

2.2 Bluetooth Low Energy Advances from PHY Layer

The Bluetooth Low Energy PHY specification uses the same Gaussian FSK (GFSK) modulation method as the Basic Rate. Its principal objective was to extend PHY-layer related functions while minimizing hardware changes. Table 1 lists the separate Bluetooth Low Energy PHY specifications and features.

Table 1 PHY Additions With Each Bluetooth Core Specification

Core Spec.	PHY	Feature
to 4.2	LE 1M (BLE)	Variable data length
5.0	LE 2M (2LE) LE coded (BLR)	Faster transmission speed Longer communications distance
5.1	Constant Tone Extension (AoA/AoD)	Direction finding

There are also different PHY-layer packet formats for different Low Energy specifications as shown in Figure 2.

BLE (1 Mbps)

Preamble (1 octets)	Access-address (4 octets)	PDU (2-258 octets)	CRC (3 octets)
---------------------	---------------------------	--------------------	----------------

2LE (2 Mbps)

Preamble (2 octets)	Access-address (4 octets)	PDU (2-258 octets)	CRC (3 octets)
---------------------	---------------------------	--------------------	----------------

LE coded (1 bps)

← S=8 coding → ← S=2 or 8 coding →

Preamble (80 μs)	Access address	CI	TERM1	PDU	CRC	TERM2
------------------	----------------	----	-------	-----	-----	-------

BLE with constant tone extension (1 Mbps)

Preamble (1 octets)	Access address (4 octets)	PDU (2-258 octets)	CRC (3 octets)	Constant Tone Extension (16 to 160 μs)
---------------------	---------------------------	--------------------	----------------	--

2LE with constant tone extension (2 Mbps)

Preamble (2 octets)	Access address (4 octets)	PDU (2-258 octets)	CRC (3 octets)	Constant Tone Extension (16 to 160 μs)
---------------------	---------------------------	--------------------	----------------	--

Figure 2 Low Energy PHY-Layer Packet Formats

The 2LE specification increases the transmission rate from 1 to 2 Mbps while following the BLE packet format, excluding the Preamble. However, the number of bits allocated to the Preamble length is doubled to 2 octets so that the time length is the same to detect kind of PHY surely.

The LE coded specification achieves longer distance transmission using encoded gain by encoding data to double length or 8-times the length, excluding the Preamble. The Preamble is 10 times longer than BLE to maintain synchronization performance even at low levels.

The Direction Finding extension appends a continuous signal called the Constant Tone Extension to the end of the

normal BLE and 2LE packets (sends unmodulated signal by sending bit 1 continuously at +1 MHz relative to carrier frequency) (Figure 3).

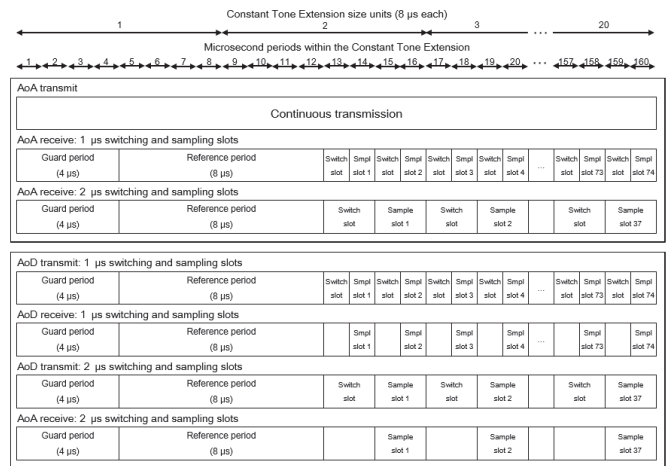


Figure 3 Constant Tone Extension Structure

2.3 Direction Finding

Direction finding using Bluetooth is achieved with combination of one or other of the multiple Tx or Rx antennas and other single antenna.

The side with multiple antennas uses timesharing when sending (or receiving) the Constant Tone Extension. The antennas are switched in order at a constant time interval (Figures 6 and 7).

The side with the single antenna just uses the conventional PHY layer to send (or receive) the signal to (or from) the multiple antennas, helping hold-down costs by using the original unmodified hardware.

Additionally, position detection indoors, etc., can be implemented by direction finding at multiple locations.

2.3.1 Direction Finding Structure

Direction finding is achieved by detecting distance differences between antennas as phase differences. Figures 4 and 5 show the detection principle for departure and arrival detection of wireless signals using a 2-antenna model.

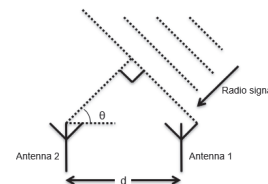


Figure 4 Arrival Direction Detection

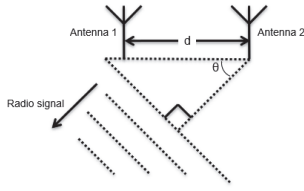


Figure 5 Departure Direction Detection

When receiving the signal sent from the single antenna at the multiple antennas, there is a difference in distance according to the arrival direction created between the multiple antennas (Figure 4). If the angle of arrival is θ , and the distance between the antennas is d , the phase difference ϕ depends on the distance difference $d\cos(\theta)$ between the antennas as:

$$\phi = 2\pi d \cos(\theta) / \lambda$$

where, λ is the signal wavelength. The angle of arrival θ at the receive side can be calculated by detecting ϕ as:

$$\theta = \arccos((\phi\lambda)/(2\pi d))$$

Conversely, when receiving the signal sent from the multiple antennas at the single antenna, there is a difference in distance corresponding to the departure direction between the Tx antennas (Figure 5). The departure direction can be found by detecting the phase difference between the antennas at the Rx side.

2.3.2 Angle of Arrival (AoA)

To detect the arrival direction, as shown in Figure 6, the Constant Tone Extension part of the signal sent by the single antenna is received by timesharing at the multiple antennas and the arrival direction is found by detecting the phase difference between antennas. In addition to using the phase difference between each antenna, the arrival direction can be found because the Rx side has prior knowledge about the antenna positional relationship and the switching interval.

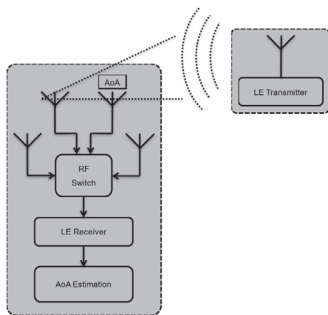


Figure 6 AoA Detection

2.3.3 Angle of Departure (AoD)

When detecting the departure direction, as shown in Figure 7, the Constant Tone Extension part of the signal sent by

timesharing from the multiple antennas is received at the single antenna and the direction is found by detecting the phase difference between the antennas. Since the Tx side sends the signal at a predetermined time interval and antenna sequence at this time, the receive side can determine from what position and which antenna the signal is being received based on the time from the packet header. The side with knowledge of the antenna positional relationship and standing order (it doesn't matter whether this is the Tx or Rx side) can find the departure direction from the phase difference between the antennas similarly to the angle of arrival based on the divided phase information.

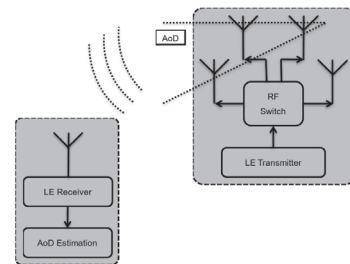


Figure 7 AoD Detection

3 AoA/AoD PHY Test Case

In both the AoA and AoD cases, the accuracy is affected by the Constant Tone Extension Tx and Rx characteristics. To assure the quality of the phase difference detection accuracy, the Bluetooth RF test specifications have added the new AoA and AoD RF test cases listed in Table 2.

Table 2 AoA/AoD Direction RF Test Items (RF-PHY.TS.p15)

Test Case #	Test Case Name
RF-PHY/TRM/BV-15-C	Output power, with Constant Tone Extension
RF-PHY/TRM/BV-16-C	Carrier frequency offset and drift, uncoded data at 1 Ms/s, Constant Tone Extension
RF-PHY/TRM/BV-17-C	Carrier frequency offset and drift at 2 Ms/s, Constant Tone Extension
RF-PHY/TRM/PS/BV-01-C	Tx Power Stability, AoD Transmitter at 1 Ms/s with 2 μ s Switching Slot
RF-PHY/TRM/PS/BV-02-C	Tx Power Stability, AoD Transmitter at 1 Ms/s with 1 μ s Switching Slot
RF-PHY/TRM/PS/BV-03-C	Tx Power Stability, AoD Transmitter at 2 Ms/s with 2 μ s Switching Slot
RF-PHY/TRM/PS/BV-04-C	Tx Power Stability, AoD Transmitter at 2 Ms/s with 1 μ s Switching Slot

Test Case #	Test Case Name
RF-PHY/TRM/ASI/BV-05-C	Antenna switching integrity, AoD Transmitter at 1 Ms/s with 2 μs Switching Slot
RF-PHY/TRM/ASI/BV-06-C	Antenna switching integrity, AoD Transmitter at 1 Ms/s with 1 μs Switching Slot
RF-PHY/TRM/ASI/BV-07-C	Antenna switching integrity, AoD Transmitter at 2 Ms/s with 2 μs Switching Slot
RF-PHY/TRM/ASI/BV-08-C	Antenna switching integrity, AoD Transmitter at 2 Ms/s with 1 μs Switching Slot
RF-PHY/RCV/IQC/BV-01-C to BV-06-C	IQ Samples Coherency
RF-PHY/RCV/IQDR/BV-07-C to BV-12-C	IQ Samples Dynamic Range

4 Functions

This section introduces the new RF test cases for AoA/AoD supported on MT8852B.

4.1 Output Power

Tx level changes in the Constant Tone Extension part have an impact on the phase-detection accuracy. This measurement evaluates the average and peak power values in the same way as conventional output power measurement by including the Constant Tone Extension part in the target measurement range. Figure 8 shows an example of the actual measurement screen. The test is for AoA transmitter.



Figure 8 Output Power Measurement Screen

4.2 Carrier Frequency Offset and Drift

Signal timesharing by antenna switching is used at phase-difference detection unlike array-antenna synchronous receiving. As a result, to keep the phase difference detection accuracy, the Constant Tone Extension part must comply with the specified frequency and the frequency deviation must be reduced.

Unlike conventional carrier frequency offset and drift which measures the frequency offset based on the Preamble

and the frequency drift according to the time variation, this measurement targets the Constant Tone Extension. This test is for AoA transmitter.

It measures the average frequencies f_0 and f_p for the Preamble and specified 16 μs at the end of the Payload (Figure 9), in addition the frequency Extension average for each 16 μs of the Constant Tone Extension (Figure 10).

Next, f_{si} ($=f_{3maxi} - \Delta f_{1avg}$) is calculated based on the mean absolute frequency shift Δf_{1avg} of the Payload part to evaluate whether each of:

$$f_{TX} - 150 \text{ kHz} \leq f_{si} \leq f_{TX} + 150 \text{ kHz} \quad *f_{TX} = \text{nominal frequency}$$

$$|f_{s1} - f_p| \leq 19.2 \text{ kHz (BLE) or } 13.6 \text{ kHz (2LE)}$$

$$|f_{si} - f_0| \leq 50 \text{ kHz}$$

$$|f_{si} - f_{si-3}| \leq 19.2 \text{ kHz}$$

is satisfied. Figure 11 shows an actual measurement screen.

When using the MT8852B, to measure in accordance with the standards, each frequency measurement position is determined by strictly detecting the symbol timing in the same manner as usual carrier frequency offset and drift.

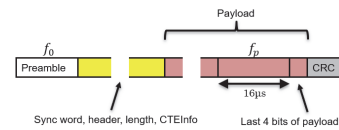


Figure 9 Constant Tone Extension Reference Frequency (f_0, f_p)

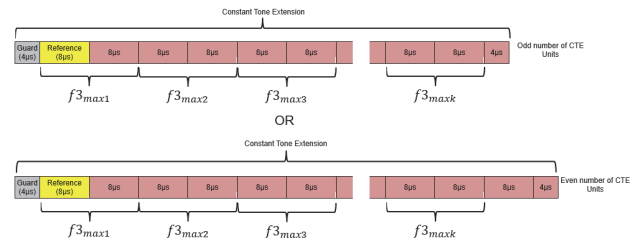


Figure 10 Constant Tone Extension Frequency Drift



Figure 11 Carrier Frequency Offset and Drift Measurement Screen

4.3 Tx Power Stability

Since AoD transmission uses time sharing by antenna switching, the switching timing and response characteristics have an impact on phase difference detection. Consequently, the Constant Tone Extension must be transmitted at a stable

fixed level during the transmission interval allocated to each antenna. Additionally, the level variation between antennas must be small.

As shown in Figure 3, the Constant Tone Extension has three intervals called the Reference period, Switch slot, and Sample slot for antenna switch timing; the antenna switching must be performed within the period of the Switch slot interval. If antenna switching exceeds the Switch slot interval, the Reference period and Sample slot intervals are affected.

When evaluating Tx Power Stability, the ratio of the measured average power $P_{REF,AVE}$ and the maximum deviation range $P_{REF,DEV}$ for the Reference period, as well as the average power $P_{n,AVE}$ of the Reference period and Sample slot, and maximum deviation range $P_{n,DEV}$ for each slot (where n is the number of each slot) must satisfy the following:

$$P_{REF,DEV}/P_{REF,AVE} < 0.25$$

$$P_{n,DEV}/P_{n,AVE} < 0.25$$

Figures 12 and 13 show some actual measurement screens.

When measuring each power using the MT8852B, the position of each measurement interval is determined accurately based on the symbol timing in the same way as carrier frequency offset and drift measurement to perform measurement in accordance with the standards. As shown in Figure 12, the worst-case value of $P_{n,DEV}/P_{n,AVE}$ for the Sample slot is displayed as the nominal value to easily show at a glance if the standard is satisfied for all Sample slots or not.

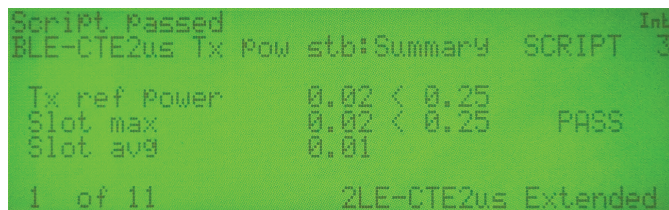


Figure 12 Tx Power Stability Measurement Screen (Reference period, Slot typical values)

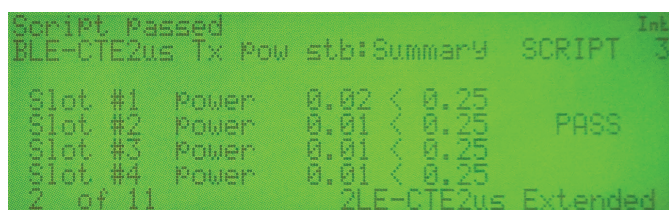


Figure 13 Tx Power Stability Measurement Screen (Each Slot)

4.4 BLE Packet Generator Expansion

The MT8852B provides a BLE packet generator function for outputting any Low Energy signal. This function has

been expanded to output AoA/AoD signals; the setting screen is shown in Figure 14.

With settings for the Constant Tone Extension type and switching time length, users can perform evaluation under desired measurement conditions, including AoA and AoD sensitivity tests that are not specified in the RF test standards.



Figure 14 BLE Packet Generator Setting Screen (CTE Settings)

5 Conclusions

This article introduces the MT8852B with an explanation of the extended Bluetooth Low Energy Direction Finding function.

As an active Bluetooth SIG member, Anritsu continues to support development of new Bluetooth technologies and standards to offer total solutions solving users' measurement questions and problems.

References

- 1) Bluetooth Core Specification revision v5.2 (2019-12)
- 2) Bluetooth Radio Frequency (RF)/Bluetooth® Test Suite revision RF.TS.p30 edition 2 (2020-1)
- 3) Bluetooth Radio Frequency Physical Layer (RF PHY)/Bluetooth® Test Suite revision RF-PHY.TS.p15 (2020-1)
- 4) Bluetooth Core Specification Version 5.2 Feature Overview version 1.0 (2020-01)

Authors



Yoshihide Goto
Product Development Dept.
IoT Test Solutions Division
Test & Measurement Company



Akihisa Kumaki
Product Development Dept.
IoT Test Solutions Division
Test & Measurement Company



Takashi Nakano
H Engineering Dept.
H Engineering Division
Test & Measurement Company

Table 3 MT8852B Support Test Cases

Basic Rate (RF.TS. p30 Rec.)	
RF/TRM/CA/BV-01-C	Output Power
RF/TRM/CA/BV-03-C	Power Control
RF/TRM/CA/BV-07-C	Modulation Characteristics
RF/TRM/CA/BV-08-C	Initial Carrier Frequency Tolerance
RF/TRM/CA/BV-09-C	Carrier Frequency Drift
RF/TRM/CA/BV-14-C	Enhanced Power Control
RF/RCV/CA/BV-01-C	Sensitivity – single slot packets
RF/RCV/CA/BV-02-C	Sensitivity – multi-slot packets
RF/RCV/CA/BV-06-C	Maximum Input Level
Enhanced Data Rate (EDR) (RF.TS. p30 Rec.)	
RF/TRM/CA/BV-10-C	EDR Relative Transmit Power
RF/TRM/CA/BV-11-C	EDR Carrier Frequency Stability and Modulation Accuracy
RF/TRM/CA/BV-12-C	EDR Differential Phase Encoding
RF/TRM/CA/BV-15-C	EDR Guard Time
RF/TRM/CA/BV-16-C	EDR Synchronization Sequence and Trailer
RF/RCV/CA/BV-07-C	EDR Sensitivity
RF/RCV/CA/BV-08-C	EDR BER Floor Performance
RF/RCV/CA/BV-10-C	EDR Maximum Input Level
Bluetooth Low Energy (RF-PHY.TS. p15 Rec.)	
RF-PHY/TRM/BV-01-C	Output power
RF-PHY/TRM/BV-05-C	Modulation Characteristics, uncoded data at 1 Ms/s
RF-PHY/TRM/BV-06-C	Carrier frequency offset and drift, uncoded data at 1 Ms/s
RF-PHY/TRM/BV-10-C	Modulation Characteristics at 2 Ms/s
RF-PHY/TRM/BV-12-C	Carrier frequency offset and drift at 2 Ms/s
RF-PHY/TRM/BV-13-C	Modulation Characteristics, LE Coded (S=8)
RF-PHY/TRM/BV-14-C	Carrier frequency offset and drift, LE Coded (S=8)
RF-PHY/TRM/BV-15-C	Output power, With Constant Tone Extension
RF-PHY/TRM/BV-16-C	Carrier frequency offset and drift, uncoded data at 1 Ms/s, Constant Tone Extension
RF-PHY/TRM/BV-17-C	Carrier frequency offset and drift at 2 Ms/s, Constant Tone Extension
RF-PHY/TRM/PS/BV-01-C	Tx Power Stability, AoD Transmitter at 1 Ms/s with 2 μ s Switching Slot
RF-PHY/TRM/PS/BV-02-C	Tx Power Stability, AoD Transmitter at 1 Ms/s with 1 μ s Switching Slot
RF-PHY/TRM/PS/BV-03-C	Tx Power Stability, AoD Transmitter at 2 Ms/s with 2 μ s Switching Slot
RF-PHY/TRM/PS/BV-04-C	Tx Power Stability, AoD Transmitter at 2 Ms/s with 1 μ s Switching Slot
RF-PHY/RCV/BV-01-C	Receiver sensitivity, uncoded data at 1 Ms/s
RF-PHY/RCV/BV-06-C	Maximum input signal level, uncoded data at 1 Ms/s
RF-PHY/RCV/BV-07-C	PER Report Integrity, uncoded data at 1 Ms/s
RF-PHY/RCV/BV-08-C	Receiver sensitivity at 2 Ms/s
RF-PHY/RCV/BV-12-C	Maximum input signal level at 2 Ms/s
RF-PHY/RCV/BV-13-C	PER Report Integrity at 2 Ms/s
RF-PHY/RCV/BV-26-C	Receiver sensitivity, LE Coded (S=2)
RF-PHY/RCV/BV-27-C	Receiver sensitivity, LE Coded (S=8)
RF-PHY/RCV/BV-30-C	PER Report Integrity, LE Coded (S=2)
RF-PHY/RCV/BV-31-C	PER Report Integrity, LE Coded (S=8)

Publicly available